



J. Serb. Chem. Soc. 78 (1) 39–55 (2013)
JSCS-4394

Metal complexes of *N'*-[2-hydroxy-5-(phenyldiazenyl)-benzylidene]isonicotinohydrazide. Synthesis, spectroscopic characterization and antimicrobial activity

ABDOU S. EL-TABL^{1*}, MOHAMAD M. E. SHAKDOFA^{2,3}
and ADEL M. E. SHAKDOFA¹

¹Department of Chemistry, Faculty of Science, El-Menoufia University, Shebin El-Kom, Egypt, ²Inorganic Chemistry Department, National Research Center, P. O. Box 12622, Dokki, Cairo, Egypt and ³Department of Chemistry, Faculty of Sciences and Arts, King Abdulaziz University, Khulais, Saudi Arabia

(Received 7 March 2011, revised 12 June 2012)

Abstract: A new series of Cu(II), Ni(II), Co(II), Mn(II), Zn(II), Cd(II), Hg(II), VO(II), UO₂(II), Fe(III) and Ru(III) complexes of *N'*-[2-hydroxy-5-(phenyldiazenyl)benzylidene]isonicotinohydrazide (H₂L) was synthesized and characterized by elemental analysis, ¹H-NMR, IR, UV-Vis and ESR spectroscopy, magnetic and thermogravimetric (TG) analyses, and conductivity measurements. The spectral data showed that the ligand behaved as a neutral bidentate (complexes **2**, **4–6** and **14**), monobasic bidentate (complexes **7** and **9**), monobasic tridentate (complexes **3**, **8**, **10**, **11** and **16**) or dibasic tridentate (complexes **12**, **13** and **15**) and was bonded to the metal ions *via* the carbonyl oxygen atom in the ketonic or enolic form, the azomethine nitrogen atom and/or the deprotonated phenolic hydroxyl oxygen. The ESR spectrum of the solid vanadyl(II) complex **2** showed an axially anisotropic spectrum with eight lines in the low field region and with $g_{\perp} > g_{\parallel}$ and $A_{\parallel} \gg A_{\perp}$ relationships, which are characteristics of a distorted octahedral structure with a d_{xy} ground state. However, the copper(II) complexes **4–6**, and the manganese(II) complex **10** showed an isotropic type symmetry, while the copper(II) complexes **3** and **7** showed an axial symmetry type with $g_{\parallel} > g_{\perp} > g_e$, indicating a covalent bond character. The antibacterial and antifungal activities of the ligand and its metal complexes showed low activity compared with the standard drugs (tetracycline for the bacteria and amphotericin B for the fungi).

Keywords: metal complexes; syntheses; spectral; isonicotinohydrazide; biological activities.

*Corresponding author. E-mail: asaeltabl@yahoo.com
doi: 10.2298/JSC110307062E

INTRODUCTION

There has been growing interest in studying hydrazones and their metal complexes due to their application as antifungal,¹⁻³ antibacterial,¹⁻⁴ anticonvulsant,⁵ anti-inflammatory,³ antimalarial,⁶ analgesic,⁷ antiplatelets,⁸ antituberculosis,⁹ anticancer activities,¹⁰ and their use in the treatment of leprosy and mental disorder diseases.¹¹ Hydrazones act as herbicides, insecticides, nematocides, rodenticides and plant growth regulators, plasticizers and stabilizers for polymers, and polymerization initiators and antioxidants. In analytical chemistry, hydrazones are used in the detection, determination and isolation of compounds containing a carbonyl group. More recently, they have been extensively used for the detection and determination of several metals.¹² Metal complexes of 2-acetylpyridine benzoylhydrazone were synthesized and crystallographically characterized.¹³ The Mn(II), Fe(III), Ni(II), Co(II) and Zn(II) complexes of 2,6-diformyl-4-methylphenol bis(benzoylhydrazone) were prepared and characterized by elemental and spectroscopic measurements.¹⁴ The Co(II), Mn(II), Cu(II) complexes of 2-acetylpyridine salicyloylhydrazone and 2-benzoylpyridine salicyloylhydrazone were also synthesized and characterized.¹⁵ Moreover, zinc(II) complexes of 2-benzoylpyridinephenylhydrazone, 2-benzoylpyridinepara-chlorophenylhydrazone and 2-benzoylpyridinepara-nitrophenylhydrazone were prepared and characterized by elemental, spectral and single-crystal X-ray diffraction analyses.¹⁶ Much work on metal complexes of hydrazones with different functional groups has been reported.¹⁷ However, little research has been devoted to metal complexes of azohydrazone ligands; hence, the synthesis, characterization and antimicrobial activities of copper(II), nickel(II), cobalt(II), manganese(II), zinc(II), cadmium(II), mercury(II), vanadyl(II), uranyl(II), iron(III) and ruthenium(III) complexes of *N'*-[2-hydroxy-5-(phenyldiazenyl)benzylidene]isonicotinohydrazide were undertaken in the reported study.

EXPERIMENTAL

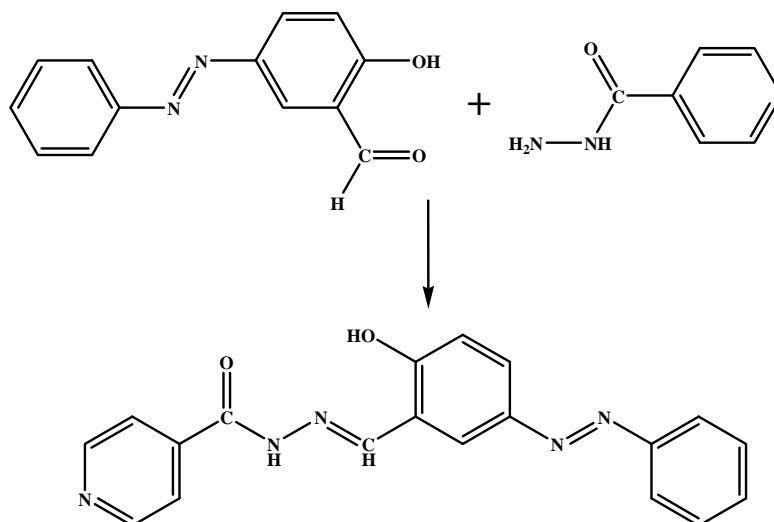
Materials and measurements

The starting chemicals were of analytical grade and provided by Merck. 2-Hydroxy-5-(phenyldiazenyl)benzaldehyde was prepared by a published method.¹⁸ Elemental analyses were determined by the Analytical Unit of the Cairo University of Egypt. Standard analytical methods were used to determine the metal ion contents.¹⁹ All metal complexes were dried in vacuum over anhydrous CaCl₂. The IR spectra were measured as KBr discs using a JASCO FT/IR 6100 spectrophotometer (400–4000 cm⁻¹). The electronic spectra in dimethyl sulfoxide (DMSO) solutions (10⁻³ M) were recorded on a Perkin-Elmer 550 spectrophotometer. The molar conductance of 10⁻³ M solutions of the complexes in DMSO was measured at 25 °C with a Bibby conductometer type MCI. The resistance measured in ohms and the molar conductivities were calculated according to the equation: $A_M = VKg/M_w R_\Omega$, where: A_M is the molar conductivity (Ω⁻¹ cm² mol⁻¹), V is the volume of the complex solution (mL), K is the cell constant (0.92 cm⁻¹), M_w is the molecular weight of the complex, g is the weight of the complex (g), R_Ω is the resistance (Ω). The ¹H-NMR spectra were recorded in DMSO-*d*₆-using

a JEOL EX-270 MHz FT-NMR spectrometer. The mass spectrum was recorded using a JEOL JMS-AX-500 mass spectrometer provided with a data system. The thermal analysis (TG) was performed under nitrogen on a Shimadzu DT-30 thermal analyzer from 23–800 °C at a heating rate of 10 °C min⁻¹. The magnetic moments (μ_B) were measured at room temperature by the Gouy method $\mu_{\text{eff}} = 2.84(\chi_{\text{m,corr}}T)^{1/2}$ using mercuric tetracyanocobaltate(II) as the magnetic susceptibility standard. Diamagnetic corrections were estimated from the Pascal constant.²⁰ ESR Measurements of the solid complexes at room temperature were realized using a Varian E-109 spectrophotometer, with di(phenyl)-(2,4,6-trinitrophenyl)imino-azanium (DPPH) as the standard material. Thin layer chromatography (TLC) was used to confirm the purity of the compounds.

Preparation of ligand [H_2L]

The ligand, *N'*-[2-hydroxy-5-(phenyldiazenyl)benzylidene]isonicotinohydrazide (H_2L) was prepared (Scheme 1) by adding equimolar amounts of isonicotinic hydrazide (1.37 g, 1.0 mmol, in 20 mL of absolute ethanol) to 2-hydroxy-5-(phenyldiazenyl)benzaldehyde (2.26 g, 1.0 mmol, in 20 mL of absolute ethanol). The mixture was refluxed under stirring for 1 h. The solid product which formed was filtered off, washed with cold ethanol, followed by crystallization from ethanol and finally dried under vacuum over anhydrous $CaCl_2$.



Scheme 1. Preparation of the ligand, *N'*-[2-hydroxy-5-(phenyldiazenyl)benzylidene]isonicotinohydrazide (H_2L).

Preparation of the metal complexes 2–16

The metal complexes were prepared by mixing a hot ethanolic solution of the required metal acetate: $Cu(CH_3COO)_2 \cdot H_2O$, $Ni(CH_3COO)_2 \cdot 4H_2O$, $Co(CH_3COO)_2 \cdot 4H_2O$, $Mn(CH_3COO)_2 \cdot 4H_2O$, $Zn(CH_3COO)_2 \cdot 2H_2O$, $Cd(CH_3COO)_2 \cdot 2H_2O$, $Hg(CH_3COO)_2 \cdot H_2O$, and $UO_2(CH_3COO)_2 \cdot H_2O$, metal chloride: $CuCl_2 \cdot 2H_2O$, $FeCl_3 \cdot 6H_2O$, $RuCl_3 \cdot 3H_2O$ or metal sulphate: $CuSO_4 \cdot 5H_2O$, $VOSO_4 \cdot H_2O$ and $Cu(NO_3)_2 \cdot 2.5H_2O$ with a suitable amount of a hot ethanolic solution of the ligand to form 1:1 or 1:2, M:L (metal:ligand) complexes in the

presence of 2 mL of triethylamine (TEA). The reaction mixture was then refluxed for a time depending on the metal salt used (2–4 h). The formed precipitates were filtered off, washed with ethanol, then with diethyl ether and dried under vacuum over anhydrous CaCl_2 .

In vitro antibacterial and antifungal activities

The biological activities of the newly synthesized hydrazone ligand, its metal complexes and metal salts were performed in the Botany Department, Laboratory of Microbiology, Faculty of Science, El-Menoufia University, Egypt. They were studied for their antibacterial and antifungal activities by the disc diffusion method.^{21,22} The antimicrobial activities were realized using the bacteria *Escherichia coli* and *Bacillus subtilis*, and the fungus *Aspergillus niger* at 10 mg mL⁻¹ concentrations in DMSO. The bacteria were subcultured in nutrient agar medium which contained 5 g L⁻¹ NaCl, 5 g L⁻¹ peptone, 3 g L⁻¹ beef extract and 20 g L⁻¹ agar in distilled water. The fungus was subcultured in Dox medium which contained (in distilled water): 1 g L⁻¹ yeast extract, 30 g L⁻¹ sucrose, 3 mg L⁻¹ NaNO_3 , 20 g L⁻¹ agar, 0.5 g L⁻¹ KCl, 1 g L⁻¹ KH_2PO_4 , 0.5 g L⁻¹ $\text{MgSO}_4 \cdot 7\text{H}_2\text{O}$ (0.5 g) and a trace of $\text{FeCl}_3 \cdot 6\text{H}_2\text{O}$ in distilled water. These mediums were then sterilized by autoclaving at 120 °C for 15 min. After cooling to 45 °C, the medium was poured into 90 mm diameter Petri dishes and incubated at 37 or 28 °C, for the bacteria and the fungus, respectively. After a few hours, the Petri dishes were stored at 4 °C. The micro-organisms were spread over each dish using a sterile bent loop rod. The test was performed by placing filter paper disks (3 mm diameter) with a known concentration of the compounds on the surface of the agar plates inoculated with a test organism. DMSO was used as the negative control. The standard antibacterial drug tetracycline, antifungal drug amphotericin B and solution of metal salts were also screened under similar conditions for comparison. The Petri dishes were incubated for 48 h at 37 or 28 °C for the bacteria and the fungus, respectively. The zone of inhibition was carefully measured in millimetres. All determinations were made in duplicate for each of the compounds. The average of the two independent readings for each compound was recorded.

RESULTS AND DISCUSSION

The ligand, *N*'-[2-hydroxy-5-(phenyldiazenyl)benzylidene]isonicotinohydrazide (H_2L) and its metal complexes **2–16** are stable at room temperature. They are non-hygroscopic and insoluble in common organic solvents, such as ethanol, methanol, chloroform and acetone, but completely soluble in DMF and DMSO. The elemental analyses showed that the complexes **3–6**, **8**, **10**, **11**, **14** and **16** were formed in a 2L:1M molar ratio, while the complexes **2**, **7**, **9**, **12**, **13** and **15** were formed in a 1L:1M molar ratio. The ¹H-NMR, IR and UV–Vis spectral data were compatible with the suggested structures (Figs. 1–3). The physical, analytical and spectral data for the ligand and its metal complexes are given in the Supplementary material to this paper, together with selected spectra of the ligand and its complexes, *i.e.*, the IR spectra of **1**, **6** and **8** (Figs. S-1–S-3), the ¹H-NMR spectra of **1** and **13** (Figs. S-4 and S-5), the mass spectrum of **1** (Fig. S-6) and the ESR spectra of **2**, **3** and **6** (Figs. S-7–S-9).

Infrared spectra

The spectrum of the ligand (H_2L) showed a strong band at 1658 cm⁻¹ due to the carbonyl group of the hydrazide moiety, whereas the medium band at 3174

cm^{-1} may be assigned to the N–H group.^{23,24} This observation indicates that the ligand is present in the ketonic form in the solid state.²⁵ The spectrum showed two broad bands in the $3300\text{--}3550\text{ cm}^{-1}$ and $2550\text{--}3000\text{ cm}^{-1}$ ranges which may be assigned to the stretching vibration of the phenolic hydroxyl groups associated through intra- and intermolecular hydrogen bonding.²³ The relatively strong and medium bands located at 1605 , 1468 and 1004 cm^{-1} corresponded to the azomethine group,²⁶ the azo group²⁷ and $\nu(\text{N--N})$,²³ respectively. The band which appeared at 1289 cm^{-1} is due to the $\nu(\text{C--OH})$ of the phenolic moiety.²⁵

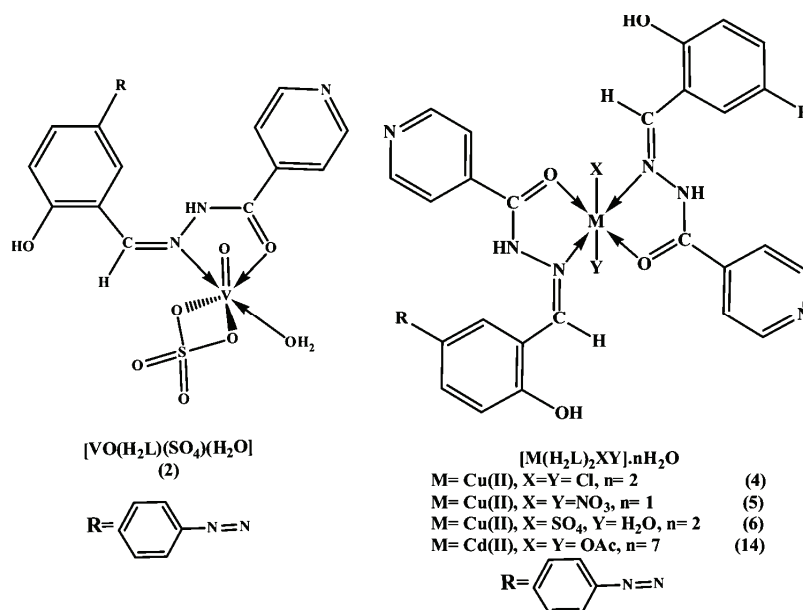


Fig. 1. Structure of the vanadyl(II), copper(II) and cadmium(II) complexes (2, 4–6 and 14, respectively).

By comparison of the spectra of the complexes with that of the free ligand, the mode of bonding between the ligand and the metal ions could be established. The spectra of complexes **7**, **9**, **12**, **13**, and **15** showed the disappearance of bands that are characteristic to $\nu(\text{C=O})$ and $\nu(\text{N--H})$, indicating that the ligand bonded to the metal ions in its enolate form through the enolic carbonyl oxygen atom. This mode of bonding was supported by the appearance of new bands in the $1507\text{--}1546\text{ cm}^{-1}$ and $1207\text{--}1258\text{ cm}^{-1}$ ranges, corresponding to $\nu(\text{N=C--O})$ and $\nu(\text{C--O})$, respectively.²⁸ In the case of complexes **2–6**, **8**, **10**, **11**, **14** and **16**, the band characteristic of $\nu(\text{N--H})$ was still present and the band of the carbonyl group was shifted to lower frequencies by $43\text{--}52\text{ cm}^{-1}$ indicating that, the ligand in these complexes coordinated to the metal ions in its ketonic form *via* the oxy-

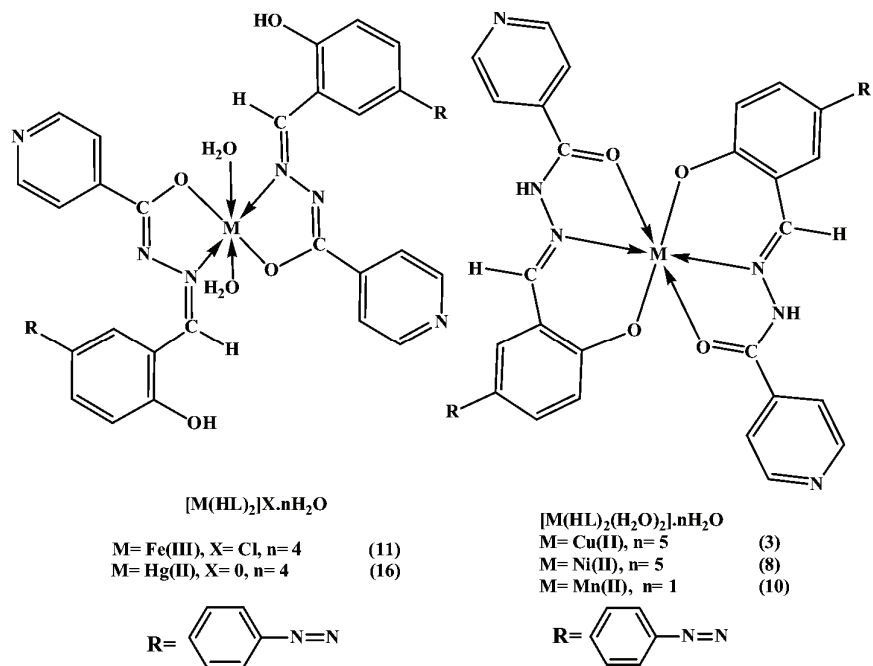


Fig. 2. Structure of the copper(II), nickel(II), manganese(II), iron(III) and mercury complexes (3, 8, 10, 11 and 16, respectively).

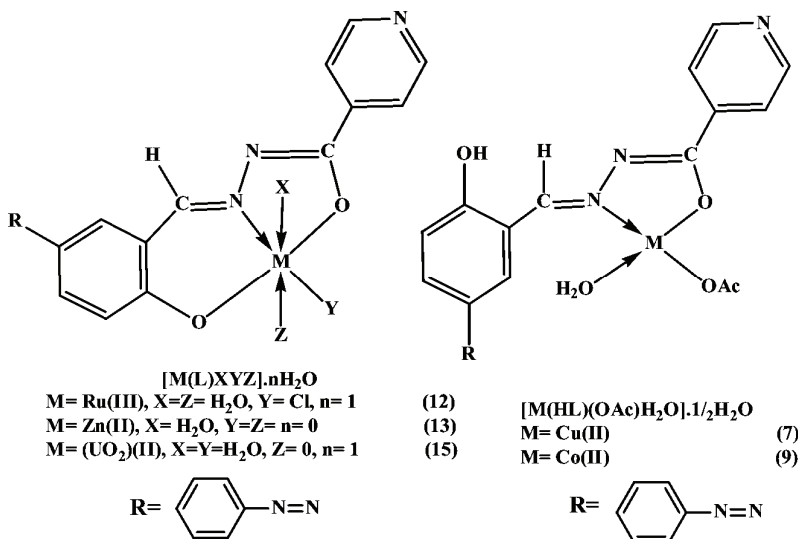


Fig. 3. Structure of the copper(II), cobalt(II), ruthenium(III), zinc(II) and uranyl(II) complexes (7, 9, 12, 13 and 15, respectively).

gen atom of the carbonyl group. In all complexes, the band characteristic of the azomethine group was shifted to lower frequencies, appearing in the 1538–1603 cm^{-1} range. At the same time, the band due to $\nu(\text{N}-\text{N})$ was shifted to a higher frequency. The increasing in the frequency of this band $\nu(\text{N}-\text{N})$ is a clear indication that an increase in the double bond character is compensating for the loss of electron density *via* electron donation to the metal ions, which is further confirmation of the coordination of the ligand *via* the azomethine group. In complexes **3**, **8**, **10–13**, **15** and **16**, the small shifts in the band characteristic of the phenolic oxygen atom indicate that the bonding occurred *via* the deprotonated phenolic oxygen atom. The appearance of new bands in the 573–610 cm^{-1} , 510–575 cm^{-1} and 467–509 cm^{-1} ranges for complexes **2–16** may be assigned to the $\nu(\text{M}-\text{O})$, $\nu(\text{M}-\text{O})$ and $\nu(\text{M}-\text{N})$, respectively.²⁹ The appearance of these bands was taken as confirmation that the bonding of the ligand with the metal ions occurred *via* the carbonyl oxygen atom in the enolic or ketonic form, azomethine nitrogen atom and/or the deprotonated phenolic hydroxyl oxygen atom. The IR spectrum of the nitrate complex (**5**) showed bands at ν_5 (1415), ν_1 (1330) and ν_2 (954), indicating that the nitrate group coordinated to the metal ion. The difference between the two high bands ($\nu_5-\nu_1$) was 85 cm^{-1} indicating that the nitrate ion bonded to the copper(II) ion in an unidentate manner.^{30–32} In the case of sulphate complexes **2** and **6**, new bands appeared at 1258, 1143, 1112 and 984 cm^{-1} , and at 1192, 1058 and 962 cm^{-1} for the two complexes, respectively. The bands of the first complex **2** indicated that the sulphates were coordinated to the vanadyl(II) ion in a chelating bidentate fashion,^{30,33} while the bands of complex **6** indicated that the sulphates were coordinated to the copper(II) ion in a chelating unidentate fashion.^{30,32} In the acetate complexes, the acetates may be coordinated to the metal ion in unidentate, bidentate or bridging bidentate manner. The $\nu_{\text{as}}(\text{CO}_2^-)$ and $\nu_{\text{s}}(\text{CO}_2^-)$ of the free acetate ion are at *ca.* 1560 and 1416 cm^{-1} respectively. In the unidentate acetate complexes, $\nu(\text{C}=\text{O})$ was higher than $\nu_{\text{s}}(\text{CO}_2^-)$ and $\nu(\text{C}-\text{O})$ was lower than $\nu_{\text{as}}(\text{CO}_2^-)$. As a result, the separation between the two $\nu(\text{C}-\text{O})$ was much larger in the unidentate than in the free ion but in the bidentate, the separation was lower than in the free ion while in the bridging bidentate, the two $\nu(\text{CO})$ were closer to the free ion.³⁰ In the case of complexes **7**, **9** and **14** two new bands appeared in the 1546–1561 cm^{-1} and 1358–1387 cm^{-1} ranges, which were attributed to the symmetric and asymmetric stretching vibration of the acetate group. The difference between these two bands are in the 159–194 cm^{-1} range, which indicates that the acetates coordinate to the metal ion in a unidentate manner.^{30,34} The infrared spectra of the vanadyl and uranyl complexes **2** and **15** revealed a medium band at 997 and 910 cm^{-1} , which may be attributed to $\nu(\text{V}=\text{O})$ ³⁵ and $\nu(\text{O}=\text{U}=\text{O})$,²⁹ respectively.

¹H-NMR spectra

The ¹H-NMR spectrum of the ligand (H₂L) shows the absence of the signal of the amino group (NH₂) characteristic of the starting material (hydrazide). The spectrum shows three sets of peaks, the first one observed as singlet at 12.41 (s, 1H) and 11.65 (s, 1H) ppm which may be assigned to the hydroxyl (OH) and (NH) protons, respectively.^{23,24,36} These hydrogen resonances appear at high δ values because of their attachment to highly electronegative atoms, oxygen and nitrogen, respectively; hence, they are in a low electron density environment. This assignment was confirmed by the deuterated spectra in which the intensity of these bands was considerably decreased. The position of these peaks in the downfield region indicates the possibility of extensive hydrogen bonding involving these groups.³⁶ The second set appeared as a singlet at 8.60 (1H, s) ppm and corresponded to the azomethine proton (H-C=N).³⁶ The third group appeared as multiplets in the 7.14–8.31 (12H, m) ppm range, which were attributed to aromatic protons. It is clear from the ¹H-NMR spectrum of the ligand that it exists in the keto form only with no evidence for the presence of the enol form. This result was confirmed by the appearance of the signal of the (NH) and phenolic (OH) only and the absence of the (OH) signal of the enolic form. The same conclusion was reported by many authors.^{24,36}

Comparing the ¹H-NMR spectra of the zinc(II) and uranyl(II) complexes, **13** and **15**, respectively, with that of the free ligand, it could be noticed that the signals of the NH and OH groups had disappeared, indicating that the ligand bonded to the zinc(II) and uranyl(II) ions as a dibasic ligand *via* the enolic carbonyl oxygen and the deprotonated hydroxyl oxygen atoms. This observation was confirmed by the absence of the signal of the acetate proton. A significant downfield shift of the azomethine proton signal in the complexes relative to the corresponding signal of the free ligand confirmed the coordination of the azomethine nitrogen atom.

Mass spectra

The mass spectrum of the ligand (H₂L) revealed a molecular ion peak at m/z 345, which is consistent with the formula weight (345.36) for this ligand. This result confirmed the identity of the ligand structure.

Molar conductivity

The molar conductivity of 1×10^{-3} M solution of the metal complexes in DMSO at room temperature are in the 3.5–22.5 $\Omega^{-1} \text{ cm}^2 \text{ mol}^{-1}$ range, except for complex **11**, indicating the non-electrolytic nature of these complexes. These results confirmed that the anion is coordinated to the metal ion. The considerably high values of some complexes may be due to partial solvolysis by DMSO. However, complex **11** has a molar conductivity value of 80.5 $\Omega^{-1} \text{ cm}^2 \text{ mol}^{-1}$, indi-

cating the electrolytic nature of this complex.³⁷ These data are in agreement with the results of Greenwood *et al.*³⁸ They suggested $50\text{--}70\ \Omega^{-1}\text{ cm}^2\text{ mol}^{-1}$ as the range for a 1:1 electrolyte in DMSO.

Electronic absorption spectra

The structure of the ligand reveals that the two lone pairs of electrons of the azo group are not the only interacting non-bonding electrons, since the hydrazone part of the ligand also contains nitrogen and oxygen atoms, which may be extra sources of lone pair of electrons. Thus, another $n\rightarrow\pi^*$ transition is expected to occur from these non-bonding orbitals to different π^* molecular orbitals extending over such large molecules.³⁹ The electronic absorption spectral bands of the ligand and its metal complexes in DMSO in the 200–1100 nm range are reported in the Supplementary material to this article. The data reveals that the spectrum of the ligand comprises three sets of bands in the UV and visible regions. The first set of shortest wavelength appeared at 270 and 320 nm and may be assigned to the $\pi\rightarrow\pi^*$ transition in the benzenoid and pyridine moieties and the intra ligand $\pi\rightarrow\pi^*$ transition.^{24,40} The second set appears at 350 and 375 nm and may be assigned to $n\rightarrow\pi^*$ of the azomethine and carbonyl group.^{24,40} The third set located at 420 nm may correspond to $\pi\rightarrow\pi^*$ transition involving the π -electrons of the azo group.^{39,41} The band located in the visible region at 455 nm can be assigned to $\pi\rightarrow\pi^*$ transition involving the whole electronic system of the compounds with a considerable charge transfer character arising mainly from the phenolic moiety.^{39,41}

The spectrum of vanadyl(II) complex **2** in DMSO solution showed that there are three bands at 700, 575 and 520 nm, which may be assigned to ${}^2B_2(d_{xy})\rightarrow E(d_{xz}, d_{zy})$, ${}^2B_2(d_{xy})\rightarrow {}^2B_1(d_{x^2-y^2})$ and ${}^2B_2(d_{xy})\rightarrow {}^2A_1(d_{z^2})$ transitions, indicating that the vanadyl(II) complex has a distorted octahedral structure (Fig. 1).^{42–44} The spectra of copper(II) complexes **3–6** were nearly identical, showing a broad band centered in the 630–675 nm range. The position and the broadness of this band indicated that copper(II) ion has a tetragonally distorted octahedral geometry (Figs. 1 and 2). This broad band may consist of three superimposed transitions ${}^2B_{1g}\rightarrow {}^2E_g$, ${}^2B_{1g}\rightarrow {}^2A_{1g}$ and ${}^2B_{1g}\rightarrow {}^2B_{2g}$.^{42,45} This could be due to the Jahn Teller effect that operates on the d^9 electronic ground state of six-coordinated system, elongating one *trans* pair of coordinate bonds and shortening the remaining four. However, the electronic spectrum of the copper complex **7** showed a broad band with shoulders at 650 and 730 nm. This spectrum is similar to that reported for square planar copper(II) complexes (Fig. 3).^{42,46} The electronic spectrum of the nickel(II) complex **8** exhibited three bands located at 850 (ν_1), 660 (ν_2) and 580 (ν_3) nm, which may be assigned to ${}^3A_{2g}\rightarrow {}^3T_{2g}$, ${}^3A_{2g}\rightarrow {}^3T_{1g}$ and ${}^3A_{2g}\rightarrow {}^3T_{1g}(p)$ spin-allowed transitions, respectively, which are characteristic of the nickel(II) ion in an octahedral structure (Fig. 2).^{42,45–48} The

ν_2/ν_1 ratio of 1.29 is lower than the usual range 1.50–1.75, indicating a distorted nickel(II) complex.⁴⁸ The electronic spectrum of the cobalt(II) complex **9** showed two bands appearing at 650 and 505 nm. These bands may be assigned to $^4A_2(F) \rightarrow ^4T_{1g}(p)$ transitions, suggesting that a tetrahedral geometry around the cobalt(II) ion (Fig. 3).^{42,49} This assignment is supported by the μ_{eff} value 4.42 μ_B , which is consistent with a tetrahedral structure.⁴⁹ A weak band at 590 nm may be due to spin–spin coupling.⁴⁹ The electronic absorption spectrum of manganese(II) complex **10** displayed weak absorption bands at 650, 600, 540 and 465 nm. These bands may corresponded to $^6A_{1g} \rightarrow ^4T_{1g}(^4G)$ (ν_1), $^6A_{1g} \rightarrow ^4E_g(^4G)$ (ν_2), $^6A_{1g} \rightarrow ^4E_g(^4D)$ (ν_3) and $^6A_{1g} \rightarrow ^4T_{1g}(^4p)$ (ν_4) transitions, respectively. These transitions are characteristic of a manganese(II) ion in an octahedral geometry (Fig. 2).⁵⁰ The electronic absorption spectrum of iron(III) complex **11** showed bands at 640 and 580 nm, which may be assigned to $^6A_{1g} \rightarrow ^4T_{2g}(G)$ and $^6A_1(G) \rightarrow ^4T_1(G)$ transitions, respectively. These bands are characteristic of an octahedral iron(III) complex (Fig. 2).⁵¹ However, the electronic absorption spectrum of ruthenium(III) complex **12** in DMSO solution displayed two bands, at 560 and 650 nm. The first band is due to a ligand-to-metal charge-transfer (LMCT) transition and the second is assigned to a $^2T_{2g} \rightarrow ^2A_{2g}$ transition. The band positions are similar to those observed for other octahedral ruthenium(III) complexes (Fig. 3).⁵² The electronic spectrum of the uranyl complex **15** exhibits one band at 530 nm which may be assigned to ligand-to-uranium charge-transfer transitions (Fig 3).⁵³ The diamagnetic zinc(II), cadmium(II) and mercury(II) complexes (**13**, **14** and **16**) have a d^{10} system, so they do not show d–d transitions.

Magnetic moments

The magnetic moments of the complexes **2–16** at room temperature are presented in the Supplementary material to this article. The results showed that all these complexes **2–12** are paramagnetic. The vanadyl complex **2** shows a magnetic value equal to 1.73 μ_B , which corresponds to one unpaired electron.^{28,32} The copper(II) complexes **3–7** showed values in the 1.68–1.88 μ_B range, which are consistent with a one-unpaired electron system in an octahedral or square planar structure.²⁴ The nickel(II) complex **8** showed a value of 3.01 μ_B , which is consistent with a two-unpaired electron system of an octahedral nickel(II) complex.²⁴ The cobalt(II) complex **9** showed a value of 4.42 μ_B ; this value indicates a high-spin tetrahedral cobalt(II) complex.⁴⁹ The magnetic moment values of the manganese(II) complex **10** and iron(III) complex **11** are 4.87 and 5.34 μ_B , respectively. These values are compatible with high-spin manganese(II) and iron(III) complexes, respectively.⁴⁰ The magnetic moment value of ruthenium(III) complex **12** is 1.65 μ_B , which is characteristic for a d^5 low-spin ruthenium(III) complex.⁴⁰

Electron spin resonance of the copper(II), nickel(II), cobalt(II), manganese(II) and vanadyl(II) complexes

The ESR spectrum of the solid vanadyl(II) complex **2** (d^1 , ^{51}V , $I = 7/2$) is an axially anisotropic eight-line spectrum with $g_{\perp} > g_{\parallel}$ and $A_{\parallel} \gg A_{\perp}$ relationships, which are characteristics of a distorted octahedral structure with a d_{xy} ground state.⁵⁴ The spectrum shows two types of resonance components, one set is due to parallel features (g_{\parallel}) and the other set due to perpendicular features (g_{\perp}), which indicate axially symmetric anisotropy, characteristic of interaction between the electron spin and vanadium nuclear spin. Ligand nitrogen superhyperfine splitting was not observed on vanadium line, indicating interaction occurring between the electron spin and the ligand.⁵⁵⁻⁵⁷ These values are typical for VO^{2+} in a distorted octahedral complex.^{58,59} The molecular orbital coefficients α^2 and β^2 were also calculated for the complexes using the following equations.:

$$\alpha^2 = \frac{E(2.0023 - g_{\parallel})}{8\lambda\beta^2} \quad (1)$$

$$\beta^2 = -1.17 \frac{A_{\parallel}}{P} + \frac{A_{\perp}}{P} + g_{\parallel} - 0.36g_{\perp} - 0.64g_e \quad (2)$$

where $P = 128 \times 10^{-4} \text{ cm}^{-1}$, $\lambda = 135 \text{ cm}^{-1}$ and E is the electronic transition energy of ${}^2\text{B}_2 \rightarrow {}^2\text{E}$. The lower values for α^2 compared to β^2 indicate that in-plane σ bonding is more covalent than in-plane π -bonding.⁶⁰ The in-plane π -bonding parameter β^2 observed are consistent with those observed by McGarvey and Kivelson for vanadyl complexes of acetylacetone.⁶¹

The ESR spectra of the solid copper(II) complexes **4–6** at room temperature exhibit high field signals, which are isotropic due to the tumbling motion of the molecules. The g_{iso} values of the complexes are 2.080, 2.055 and 2.104, respectively.^{32,62} The ESR spectra of the solid copper(II) complexes **3** and **7** at room temperature are characteristic for a d^9 configuration, having an axial symmetry type of a $d_{(x^2-y^2)}$ ground state, which is the most common state for copper(II) complexes.^{63,64} The g values of $g_{\parallel} = 2.235$ and 2.198, $g_{\perp} = 2.045$ and 2.056 with $g_{\text{iso}} = 2.108$ and 2.104, respectively, suggest an elongated tetragonal octahedral geometry for **3** and square planar for **7**.⁶⁵ The trend of the g -values, *i.e.*, $g_{\parallel} > g_{\perp} > g_e(2.0023)$ confirmed the tetragonal distortion around the copper(II) ion in **3** and the square planar geometry in **7**,⁶⁶ which correspond to elongation of the four-fold symmetry axis z . In addition, exchange coupling interactions between the copper(II) ion are explained by the Hathaway Expression $G = (g_{\parallel} - 2)(g_{\perp} - 2)$. If the value of G is < 4.0 , a considerable exchange coupling is present in the solid complex. If G is > 4.0 , the exchange interactions are negligible, which is typical as in the case of complexes **3** and **7** ($G = 5.22$ and 4.15, respectively). This confirmed the tetragonal octahedral and square planar structures in **3** and **7**, respec-

tively.^{67,68} Kivelson and Neiman showed that for an ionic environment, g_{\parallel} is ≥ 2.3 , but for a covalent environment $g_{\parallel} < 2.3$. The g_{\parallel} -values for complexes **3** and **7** are 2.235 and 2.225, respectively; consequentially, the environments are considerably covalent.^{67,68}

The ESR spectra of the solid nickel(II) and cobalt(II) complexes **8** and **9** at room temperature do not show any ESR signals as rapid spin lattice relaxation of nickel(II) and cobalt(II) tends to broaden the lines at higher temperatures.⁴⁰ The ESR spectra of the solid manganese(II) complex **10** and ruthenium(III) complex **12** give isotropic signals centred at 1.997 and 2.150, respectively. The broadening of the spectra is due to spin relaxation.⁴⁰ The spectrum of ruthenium(III) complex shows an additional weak signal at 2.00, which may be due to the free radical.

Thermal analysis of some of the complexes

The thermogravimetric (TG) analysis was realised in the temperature range 20–800 °C under nitrogen. The results (Table I) show good agreement between the calculated and experimental weight losses. The results showed that the complexes **2**, **5–7** and **12** generally decomposed in several steps. The first step is the elimination of water of hydration or solvent molecules, as in complexes **5–7** and **12**, in the temperature range 30–117 °C. The second step is the loss of water of coordination, as in complexes **2**, **6**, **7** and **12**, in the 100–350 °C range. The observed loss of coordinated water at high temperatures may be due to hydrogen bonding with the hydroxyl group. The third step is the loss of the anions (sulphate, nitrate, chloride and acetate) in the temperature range 240–380 °C. The fourth step is the complete decomposition of the complexes through degradation of the ligand in temperature range 300–680 °C, leaving metal oxide as the residue.

TABLE I. The results of the thermogravimetric analysis of some of the complexes

No.	Temp. range, °C	Loss in weight Found (Calcd.), %	Assignment	Composition of the residue
2	140–175	3.6 (3.4)	Loss of one molecule of coordinated water	[VO (H ₂ L) ₂ (SO ₄)]
	320–380	18.0 (18.2)	Loss of sulphate group	[VO (HL) ₂]
	400–490	66.7 (65.6)	Decomposition of the complex forming V ₂ O ₅	V ₂ O ₅
5	50–90	2.3 (2.0)	Dehydration process (H ₂ O)	[Cu(H ₂ L) ₂ (NO ₃) ₂]
	300–350	13.9 (13.8)	Loss of two nitrate groups (2HNO ₃)	[Cu(HL) ₂]
	360–680	72.2 (75.3)	Decomposition of the complex forming CuO	CuO

TABLE I. Continued

No.	Temp. range, °C	Loss in weight Found (Calcd.), %	Assignment	Composition of the residue
6	50–117	3.8 (4.0)	Dehydration process (H ₂ O)	[Cu(H ₂ L) ₂ (SO ₄)H ₂ O]
	130–260	2.0 (2.0)	Loss of one molecule of coordinated water	[Cu(H ₂ L) ₂ (SO ₄)]
	270–350	10.8 (10.6)	Loss of one sulphate group (H ₂ SO ₄)	[Cu(HL) ₂]
	370–650	57.0 (61.2)	Decomposition of the complex forming CuO	CuO
7	50–110	3.5 (3.6)	Dehydration process (H ₂ O)	[Cu(HL)(OAc)(H ₂ O)]
	205–250	3.5 (3.6)	Loss of one molecule of coordinated water	[Cu(HL)(OAc)]
	270–356	12.4 (11.3)	Loss of one acetate group (HOAc)	[Cu(L)]
	360–580	68.1 (58.6)	Decomposition of the complex forming CuO	CuO
12	50–105	3.5 (3.4)	Dehydration process (H ₂ O)	[Ru(L)Cl(H ₂ O) ₂]
	110–230	6.4 (6.7)	Loss of two molecule of coordinated water	[Ru(L)Cl]
	240–280	6.9 (6.6)	Loss of one chlorine (HCl)	[Ru(L–H)]
	300–430	56.7 (59.2)	Decomposition of the complex forming Ru ₂ O ₃	Ru ₂ O ₃

Antibacterial and antifungal screening

The results of screening of antimicrobial activities of the ligand and its metal complexes are listed in Table II. The results show that all the metal complexes exhibited inhibitory effects towards the gram-positive bacterium *B. subtilis* and the gram-negative bacterium *E. coli*. Moreover, the complexes **4** and **13–16** exhibited inhibitory effects towards the fungus *A. niger*. In comparison, the parent organic ligand and the solutions of the metal salts had low activity against the bacteria and were inactive against fungus under the experimental conditions. The order of the activity of the compounds against *B. subtilis* was tetracycline > **3** > **2** = **4** > **14** = **16** > **8** > **12** > **6** = **7** = **10** = **13** = **15** > **1** = **5** = **9** > **11**, Table II. The order of the activity against *E. coli* was **2** > tetracycline > **4** > **14** > **15** > **11** > **7** > **6** > **1** = **8** = **13** = **16** > **12** > **3** > **5** > **9** = **10**, Table II. However, the order of the activity against the fungus *A. niger* was **16** > **4** > **14** > amphotericin B = **15** > **13**, Table II. The results show that the activity of complexes against the tested micro-organisms was significantly enhanced on coordination. This enhancement in the activity may be rationalized on the basis that their structures mainly possess an additional C=N bond. The most interesting point of the biological measurements is that the azohydrazone had a mild biological effect while other types of hydrazones, such as *N*-phenylglycine 2-(1-methyl-3-oxobutylidene)hydrazide,⁶⁹ 3-hydroxy-2-naphthalenecarboxylic acid, [1-(2-pyridinyl)ethylidene]hydrazide,⁷⁰

p-aminoacetophenone isonicotinoylhydrazone² and Schiff bases^{4,71–73} are biologically strongly active. In addition, their metal complexes showed higher biological activity than the azohydrazone complexes. Hence, it may be stated that the lower activity of azohydrazone and its complexes against both bacteria and fungi could be attributed to the presence of the azo group.

TABLE II. Biological activities of the ligand and its metal complexes against bacteria and a fungus; inhibition zone, mm

Compound	<i>A. niger</i>	<i>E. coli</i>	<i>B. subtilis</i>
DMSO	0	0	0
Amphotericin B	17	–	–
Tetracycline	–	35	40
Ligand (1)	0	15	15
2	0	42	24
3	0	13	28
4	20	32	24
5	0	12	15
6	0	17	17
7	0	18	17
8	0	15	21
9	0	11	15
10	0	11	17
11	0	19	11
12	0	14	20
13	12	15	17
14	18	25	22
15	17	20	17
16	40	15	22

CONCLUSIONS

The Cu(II), Ni(II), Co(II), Mn(II), Zn(II), Cd(II), Hg(II), VO(II), UO₂(II), Fe(III) and Ru(III) complexes of *N'*-[2-hydroxy-5-(phenyldiazenyl)benzylidene]-isonicotinohydrazide (H₂L) were characterized by elemental analysis, ¹H-NMR, IR, UV–Vis and ESR spectroscopy, thermogravimetric analyses and magnetic and conductivity measurements. The analyses revealed that the ligand bonded in one of four modes, neutral bidentate, monobasic bidentate, monobasic tridentate or dibasic tridentate with the different metal ions *via* the oxygen atom of the carbonyl group in the ketonic or enolic form, the nitrogen atom of the azomethine group or the deprotonated hydroxyl oxygen atom of the azo moiety. The analytical and spectral data showed the prepared complexes had either octahedral or square planar geometry. Some of the metal complexes exhibited inhibitory effects towards gram-positive (*B. subtilis*) and gram-negative (*E. coli*) bacteria and the complexes **4**, **13**–**16** exhibited inhibitory effects towards the fungus *A. niger*.

SUPPLEMENTARY MATERIAL

Physical and spectral data of the synthesized compounds are available electronically from <http://www.shd.org.rs/JSCS/>, or from the corresponding author on request.

ИЗВОД

КОМПЛЕКСИ МЕТАЛА СА N' -[2-ХИДРОКСИ-5-(ФЕНИЛДИАЗЕНИЛ)-БЕНЗИЛИДЕН]-
-ИЗОНИКОТИНОХИДРАЗИДОМ. СИНТЕЗА, СПЕКТРОСКОПСКА
КАРАКТЕРИЗАЦИЈА И АНТИМИКРОБНА АКТИВНОСТ

ABDOU S. EL-TABL¹, MOHAMAD M. E. SHAKDOFA^{2,3} и ADEL M. E. SHAKDOFA¹

¹Department of Chemistry, Faculty of Science, El-Menoufia University, Shebin El-Kom, Egypt, ²Inorganic Chemistry Department, National Research Center, P.O. Box 12622, Dokki, Cairo, Egypt and ³Department of Chemistry, Faculty of Sciences and Arts, King Abdulaziz University, Khulais, Saudi Arabia

Синтетизована је нова серија Cu(II), Ni(II), Co(II), Mn(II), Zn(II), Cd(II), Hg(II), VO(II), UO₂(II), Fe(III) и Ru(III) комплекса са N' -[2-хидрокси-5-(фенилдиазенил)-бензилиден]-изоникотинохидразиdom (H₂L) као лигандом. За карактеризацију комплекса употребљени су елементална микроанализа, ¹H-NMR, IR, UV-Vis, ESR, термогравиметријска (TG) анализа, магнетна и кондуктометријска мерења. Спектроскопска мерења су показала да се у случају комплекса **2**, **4–6** и **14** H₂L координује као неутрални бидентатни лиганд код комплекса **7** и **9** као монобазни бидентатни лиганд, код комплекса **3**, **8**, **10**, **11** и **16** као монобазни тридентатни лиганд и код комплекса **12**, **13** и **15** као двобазни тридентатни лиганд. Координација лиганда за јон метала се одвија преко карбонилног кисеониковог атома у енолној или кето форми, азометинског атома азота, или депротонованог фенолног атома кисоника. ESR мерења ванадил(II) комплекса у чврстом стању (**2**) показују аксијално-анизотропски облик спектра са осам линија у области ниже енергије $g_{\perp} > g_{\parallel}$ и $A_{\parallel} \gg A_{\perp}$, што одговара дисторгованој октаедарској структури комплекса са d_{xy} основним стањем. Међутим, ова мерења код комплекса бакра(II) (**4–6**), као и код комплекса мангана(II) (**10**) показују изотропски облик ESR спектра, док у случају комплекса бакра(II) (**3** и **7**) ови спектри показују аксијалну симетрију са $g_{\parallel} > g_{\perp} > g_e$, што указује на присуство ковалентног карактера везе. Резултати испитивања антибактеријске и антифунгалне активности за H₂L лиганд и испитиване комплексе одговарају активности средње јачине у поређењу са стандардним агенсима.

(Примљено 7. марта 2011, ревидирано 12. јуна 2012)

REFERENCES

1. V. P. Singh, A. Katiyar, S. Singh, *Biometals* **21** (2008) 491
2. V. P. Singh, A. Katiyar, S. Singh, *J. Coord. Chem.* **62** (2009) 1336
3. K. V. Sharma, V. Sharma, R. K. Dubey, U. N. Tripathi, *J. Coord. Chem.* **62** (2009) 493
4. K. M. Ibrahim, I. M. Gabr, G. M. Abu El-Reash, R. R. Zaky, *Monatsh. Chem.* **140** (2009) 625
5. Ş. G. Küçüküzümlü, A. Mazi, F. Sahin, S. Öztürk, J. Stables, *Eur. J. Med. Chem.* **38** (2003) 1005
6. P. Melnyk, V. Leroux, C. Sergheraert, P. Grellier, *Bioorg. Med. Chem. Lett.* **16** (2006) 31
7. P. C. Lima, L. M. Lima, K. C. M. da Silva, P. H. O. Léda, A. L. P. de Miranda, C. A. M. Fraga, E. J. Barreiro, *Eur. J. Med. Chem.* **35** (2000) 187

8. A. C. Cunha, J. M. Figueiredo, J. L. M. Tributino, A. L. P. Miranda, H. C. Castro, R. B. Zingali, C. A. M. Fraga, M. C. B. V. de Souza, V. F. Ferreira, E. J. Barreiro, *Bioorg. Med. Chem.* **11** (2003) 2051
9. K. K. Bedia, O. Elçin, U. Seda, K. Fatma, S. Nathaly, R. Sevim, A. Dimoglo, *Eur. J. Med. Chem.* **41** (2006) 1253
10. N. Terzioglu, A. Gürsoy, *Eur. J. Med. Chem.* **38** (2003) 781
11. C. Loncle, J. M. Brunel, N. Vidal, M. Dherbomez, Y. Letourneux, *Eur. J. Med. Chem.* **39** (2004) 1067
12. S. H. Guzar, J. Qin-Hang, *Chem. Res. Chin. Univ.* **24** (2008) 143
13. Y. J. Jang, U. Lee, B. K. Koo, *Bull. Korean Chem. Soc.* **26** (2005) 925
14. P. Cheng, D. Liao, S. Yan, Z. Jiang, G. Wang, *Polyhedron* **14** (1995) 2355
15. S. Shit, J. Chakraborty, B. Samanta, A. M. Z. Slawin, V. Gramlich, S. Mitra, *Struct. Chem.* **20** (2010) 633
16. A. A. Recio Despaigne, J. G. da Silva, A. C. M. do Carmo, O. E. Piro, E. E. Castellano, H. Beraldo, *Inorg. Chim. Acta* **362** (2009) 2117
17. A. S. El-Tabl, R. M. El-Bahnasawy, A. E. Hamdy, *J. Chem. Res.* (2009) 659
18. J.-N. Liu, B.-W. Wu, B. Zhang, Y. Liu, *Turk. J. Chem.* **30** (2006) 41
19. G. Svehla, *Vogel's textbook of macro and semi micro quantitative inorganic analysis*, 5th ed., Longman, New York, 1979
20. L. Lewis, R. G. Wilkins, *Modern coordination chemistry*, Interscience, New York, 1960
21. E. O. Offiong, S. Martelli, *Farmaco* **49** (1994) 513
22. *Practical Medical Microbiology*, J. G. Collee, J. P. Duguid, A. G. Farser, B. D. Marmion, Eds., Churchill Livingstone, New York, 1989
23. M. R. Maurya, S. Khurana, C. Schulzke, D. Rehder, *Eur. J. Inorg. Chem.* (2001) 779
24. R. Gup, B. Kirkan, *Spectrochim. Acta, A* **62** (2005) 1188
25. G. C. Xu, L. Zhang, L. Liu, G. F. Liu, D. Z. Jia, *Polyhedron* **27** (2008) 12
26. B. Samanta, J. Chakraborty, S. Shit, S. R. Batten, P. Jensen, J. D. Masuda, S. Mitra, *Inorg. Chim. Acta* **360** (2007) 2471
27. H. Tezcan, E. Uzluk, *Dyes Pigm.* **77** (2008) 626
28. B. Singh, P. Srivastava, *Transition Met. Chem.* **12** (1987) 475
29. Z. H. Abd El-Wahab, M. M. Mashaly, A. A. Salman, B. A. El-Shetary, A. A. Faheim, *Spectrochim. Acta, A* **60** (2004) 2861
30. K. Nakamoto, *Infrared and Raman spectra of inorganic and coordination compounds*, 3rd ed., Wiley, New York, 1977, p. 244
31. E. Katsoulakou, V. Bekiari, C. P. Raptopoulou, A. Terzis, P. Lianos, E. M. Zoupa, S. P. Perlepes, *Spectrochim. Acta, A* **61** (2005) 1627
32. S. Chandra, L. K. Gupta, *Spectrochim. Acta, A* **61** (2005) 1181
33. B. Singh, A. K. Srivastav, P. Srivastava, *Transition Met. Chem.* **13** (1988) 463
34. L. K. Gupta, U. Bansal, S. Chandra, *Spectrochim. Acta, A* **66** (2007) 972
35. P. N. Remya, C. H. Suresh, M. L. P. Reddy, *Polyhedron* **26** (2007) 5016
36. B. N. B. Raj, M. R. P. Kurup, E. Suresh, *Spectrochim. Acta, A* **71** (2008) 1253
37. W. J. Geaey, *Coord. Chem. Rev.* **7** (1971) 81
38. N. N. Greenwood, B. P. Straughan, A. E. Wilson, *J. Chem. Soc. A* (1968) 2209
39. N. M. Rageh, A. M. Abdel Mawgoud, H. M. Mostafa, *Chem. Papers* **53** (1999) 107
40. M. F. R. Fouda, M. M. Abd-Elzaher, M. M. E. Shakdofa, F. A. El Saied, M. I. Ayad, A. S. El Tabl, *J. Coord. Chem.* **61** (2008) 1983
41. R. Gup. E. Giziroglu, B. Kirkan, *Dyes Pigm.* **73** (2007) 40

42. A. B. P. Lever, *Inorganic electronic spectroscopy*, Elsevier, Amsterdam, 1968
43. R. N. Jadeja, J. R. Shah, *Polyhedron* **26** (2007) 1677
44. A. M. B. Bastos, J. G. da Silva, P. I. Da. S. Maia, V. M. Deflon, A. A. Batista, A. V. M. Ferreira, L. M. Botion, E. Niquet, H. Beraldo, *Polyhedron* **27** (2008) 1787
45. B. Graham, L. Spiccia, B. W. Skelton, A. H. White, D. C. R. Hockless, *Inorg. Chim. Acta* **358** (2005) 3974
46. R. C. Khulbe, R. P. Singh Y. K. Bhoon, *Transition Met. Chem.* **8** (1983) 59
47. S.-X. Hui, Y.-X. Zeng, L. Cun, X.-R. Gen, *Transition Met. Chem.* **20** (1995) 191
48. K. R. Krishnapriya, M. Kandaswamy, *Polyhedron* **24** (2005) 113
49. K. Gudasi, R. V. Shenoy, R. S. Vadavi, S. A. Patil, M. Nethaji, *J. Mol. Struct.* **788** (2006) 22
50. R. Sharma, S. K. Agarwal, S. Rawat, M. Nagar, *Transition Met. Chem.* **31** (2006) 201
51. M. Tiliakos, P. Cordopatis, A. Terzis, C. P. Raptopoulou, S. P. Perlepes, E. M. Zoupa, *Polyhedron* **20** (2001) 2203
52. A. N. Al-Hakimi, A. S. El-Tabl, M. M. E. Shakhdo, *J. Chem. Res.* (2009) 770
53. J. B. Gandhi, N. D. Kulkarni, *Transition Met. Chem.* **26** (2001) 96
54. G. R. Hauson, T. A. Kabanos, A. D. Keramidas, D. Mentzafos, A. Terzis, *Inorg. Chem.* **31** (1992) 2587
55. D. Kivelson, S.-K. Lee, *J. Chem. Phys.* **41** (1964) 1896
56. F. A. Walker, R. L. Carlin, P. H. Rieger, *J. Chem. Phys.* **45** (1966) 4181
57. D. Kivelson, *J. Chem. Phys.* **33** (1960) 1094
58. Y. Dong, R. K. Narla, E. Sudbeck, F. M. Uckun, *J. Inorg. Biochem.* **78** (2000) 321
59. S. S. Dodward, R. S. Dhamnaskar, P. S. Prabhu, *Polyhedron* **8** (1989) 1748
60. N. Raman, Y. P. Raja, A. Kulandaisamy, *Proc. Indian Acad. Sci. (Chem. Sci.)* **113** (2001) 183
61. P. B. Sreeja, M. R. P. Kurup, *Spectrochim. Acta, A* **61** (2005) 331
62. K. B. Gudasi, R. S. Vadavi, R. V. Shenoy, S. A. Patil, M. Nethaji, *Transition Met. Chem.* **31** (2006) 374
63. A. S. El-Tabl, *Bull. Korean Chem. Soc.* **25** (2004) 1757
64. B. J. Hathaway, D. E. Billing, *Coord. Chem. Rev.* **5** (1970) 143
65. A. S. El-Tabl, *Transition Met. Chem.* **27** (2002) 166
66. A. S. El-Tabl, *Transition Met. Chem.* **23** (1998) 63
67. R. K. Ray, G. B. Kauffman, *Inorg. Chim. Acta* **174** (1990) 237
68. R. K. Ray, G. B. Kauffman, *Inorg. Chim. Acta* **174** (1990) 257
69. A. S. El-Tabl, F. A. El-Saied, A. N Al-Hakimi, *J. Coord. Chem.* **61** (2008) 2380
70. K. M. Ibrahim, I. M. Gabr, R. R. Zaky, *J. Coord. Chem.* **62** (2009) 1100
71. G. B. Bagihalli, S. A. Patil, *J. Coord. Chem.* **62** (2009) 1690
72. A. Kulkarni, P. G. Avaji, G. B. Baghialli, S. A. Patil, P. S. Badami, *J. Coord. Chem.* **62** (2009) 481
73. K. V. Sharma, V. Sharma, R. K. Dubey, U. N. Tripathi, *J. Coord. Chem.* **62** (2009) 506.

Copyright of Journal of the Serbian Chemical Society is the property of National Library of Serbia and its content may not be copied or emailed to multiple sites or posted to a listserv without the copyright holder's express written permission. However, users may print, download, or email articles for individual use.